Effect of Uniaxial Stresses on the Paramagnetic Spectra of Mn^{3+} and Fe^{3+} in MgO*

Elsa Rosenvasser Feher

University of California, San Diego, La Jolla, California

(Received 4 May 1964)

We have investigated the lowest energy levels of the paramagnetic ions Mn^{2+} and Fe^{3+} in the host crystal MgO, as a function of externally applied uniaxial stress. The effect of the stress on the energy levels of the paramagnetic ion can be described by introducing into the spin Hamiltonian an additional term of the form $S \cdot D \cdot S$. When the components of D are expressed as linear functions of the applied stress components, there are only two independent constants of proportionality in our simple case of a cubic crystalline lattice. We have experimentally determined these two constants, i.e., spin-lattice coefficients C_{11} and C_{44}, for Mn^{2+} and Fe^{3+} in MgO, and find them to be, in units of 10^{-13} cm/dyne: for Mn^{2+}, $C_{11} = (+7.1\pm3)\%$ and $C_{44} = (-2.1\pm3)\%$; for Fe^{3+}, $C_{11} = (+26\pm3)\%$ and $C_{44} = (-5.5\pm5)\%$. We have also investigated the absolute value and the angular dependence of the linewidth of the fine structure of Mn^{2+} and Fe^{3+} in MgO. We can account for these widths in terms of the spin-lattice coefficients, by assuming a random distribution of internal stresses in the host sample. We also indicate the relevance of the spin-lattice coefficients in the determination of the direct spin-lattice relaxation times.

I. INTRODUCTION

THE method of electron spin resonance has been widely used over the last two decades in the study of paramagnetic ions in crystals. The transitions that are observed reflect the surroundings of the ion and much information can be obtained from them on the symmetry of the environment of the ion and on the strength and detail of the interactions between the ion and this environment. It has been the purpose of our work to study the effect on such electron spin resonance spectra of an externally applied uniaxial stress.

The idea is the following: By means of an externally applied pressure, the atoms or ions that form the lattice are statically displaced from their equilibrium positions. This introduces a change in the crystalline electric field at the site of the unpaired electron. It is possible to express the relation between this electric field and the displacement of the ions of the lattice in terms of constants characteristic of the system under consideration, which we call spin-lattice coefficients. These coefficients then provide a direct measure of the strength of the coupling between the spins and the lattice. What information can be obtained from these spin-lattice coefficients?

Firstly, they may serve to elucidate the mechanisms that produce the splittings of the energy levels of ions placed in a crystalline environment, which are imperfectly understood theoretically. Previously, in order to study the effect on a given paramagnetic ion of the symmetry of its environment, it was necessary to change the very nature of this environment (going from, say, cubic MgO to axially symmetric Al_2O_3). Using uniaxial stresses, it is possible to choose a simple crystalline lattice and to distort it at will; the effect of such distortions on the paramagnetic ions contained in the sample will then give a better handle on the problem of the mechanisms involved.

Secondly, the spin-lattice coefficients can provide knowledge of the direct spin-lattice relaxation times T_1. In fact, the classical work in this field[1] has established that spin-lattice relaxation proceeds via the thermal modulation of the crystalline electric field at the paramagnetic ion. If, then, the electric field introduced by uniaxial stresses, were not static but were modulated with a frequency distribution given by the phonon spectrum of the substance considered, we would be reproducing the mechanism of spin-lattice relaxation. In this dynamic case it should also be possible to express the relation between electric field and ionic displacement by means of the spin-lattice coefficients and so obtain the direct spin-lattice relaxation time in terms of them. Ideally, then, it would be possible to know the direct spin-lattice relaxation time of a system by performing a uniaxial pressure experiment, which is a much simpler measurement than those usually performed.

Thirdly, we have found that the spin-lattice coefficients also provide knowledge of the state of internal stress of a crystal, which manifests itself in the linewidth of the paramagnetic transitions observed.

II. ENERGY LEVELS AND TRANSITIONS OF Mn^{2+} AND Fe^{3+} IN MgO IN THE PRESENCE OF APPLIED STRESS

A. The Spin Hamiltonian

In our work we shall be concerned with the isoelectronic ions Mn^{2+} and Fe^{3+} in the cubic field of MgO. The spectra of these systems can be described in terms of the following spin Hamiltonian:

$$\mathcal{H}_c = g\beta H \cdot S + \tfrac{1}{6}a[S_x^4 + S_y^4 + S_z^4 - \tfrac{1}{5}S(S+1)(3S^2 + 3S - 1)] + A \cdot SI.$$

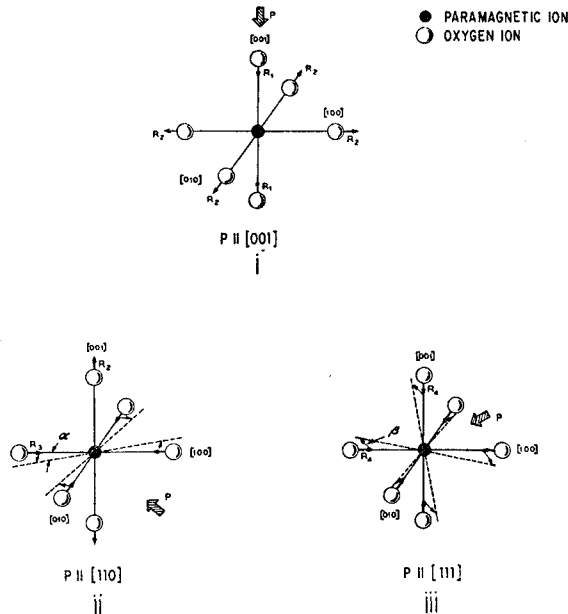[1] J. H. Van Vleck, Phys. Rev. 57, 426 (1940); R. de L. Kronig, Physica 6, 33 (1939).

FIG. 1. Distortions under stress (compression) of the octahedron formed by the six oxygens that are nearest neighbors of the paramagnetic ions considered, after Schawlow, Piksis, and Sugano (see Ref. 6). (i) $P\|[001]$; the upper and lower oxygen ions move inward by R_1; the other oxygens move outward by R_2. (ii) $P\|[110]$; the upper and lower oxygen ions move outward by R_2; the other move inward by R_3; the angle α is in the (001) plane. (iii) $P\|[111]$; all oxygen ions move inward by R_4. If $P=5.5\times10^8$ dyn/cm² ≈ 550 kg/cm², then $R_1=4.5\times10^{-4}$ Å; $R_2=1.0\times10^{-4}$ Å; $R_3=\frac{1}{2}(R_1-R_2)$; $R_4=\frac{1}{3}(R_1-2R_2)$; $\alpha=5.0\times10^{-3}$ deg; and $\beta=\frac{2}{3}\sqrt{2}\alpha$.

For Mn^{2+} the constants are[2]:

$$g=2.0014\pm0.0005; \quad 3a=(+55.9\pm0.9)\times10^{-4} \text{ cm}^{-1};$$
$$A=(-81.0\pm0.2)\times10^{-4} \text{ cm}^{-1}.$$

For Fe^{3+} the constants are[3]:

$$g=2.0037\pm0.0007; \quad 3a=+615\times10^{-4} \text{ cm}^{-1};$$

and[4]

$$A=(10.1\pm0.2)\times10^{-4} \text{ cm}^{-1}.$$

We call this spin Hamiltonian $\mathcal{3C}_c$ where the subscript indicates that it refers to the undistorted or cubic MgO lattice.

If now the MgO crystal is subjected to a uniaxial stress, the cubic symmetry is distorted, and the new spin Hamiltonian describing this system of lower symmetry becomes $\mathcal{3C}=\mathcal{3C}_c+\mathcal{3C}_{nc}$, where $\mathcal{3C}_{nc}=\sum_{i\ j=1,2,3} \times S_i D_{ij} S_j$ (1, 2, 3, denote the cubic axes of the crystal).

---

[2] W. Low, Phys. Rev. **105**, 793 (1957).

[3] W. Low, Proc. Roy. Soc. (London) **69B**, 1169 (1956).

[4] E. Rosenvasser and G. Feher, Bull. Am. Phys. Soc. **6**, 117 (1961); see also J. W. Orton, P. Auzins, J. H. E. Griffiths, and J. E. Wertz, Proc. Phys. Soc. (London) **78B**, 554 (1961); they independently also determined A. This constant describes the observed hyperfine structure due to the naturally occurring isotope Fe^{57}. Its abundance is only 2.2% and so we shall neglect it in the remainder of this paper.

We assume that no fourth-order terms in the spin variables are introduced; the validity of this assumption is shown in part B of this section.

The tensor D represents the effect of deformations (dilations and contractions) of the system, in the absence of translations, rotations or changes in volume. Such a tensor will be symmetric and traceless. In fact, like any tensor, D can be decomposed into the sum of three tensors: one antisymmetric, one symmetric and traceless, one diagonal with elements given by the trace of D. The term in $\mathcal{3C}_{nc}$ that arises from the diagonal part of D is of the form $[D_{11}+D_{22}+D_{33}] \times[S(S+1)]$, and its effect is to shift by an equal amount all energy levels belonging to the same spin multiplet. Since experimentally we observe only differences in energy, this term is not detectable and we therefore set it equal to zero; i.e., $D_{11}+D_{22}+D_{33}=0$, or D_{ij} is traceless. The antisymmetric part of D gives rise to terms linear in the spin operator. Since the system is to be invariant under time reversal, these terms must vanish. Hence $D_{ij}=D_{ji}$ and only the symmetric, traceless part of the tensor D remains.
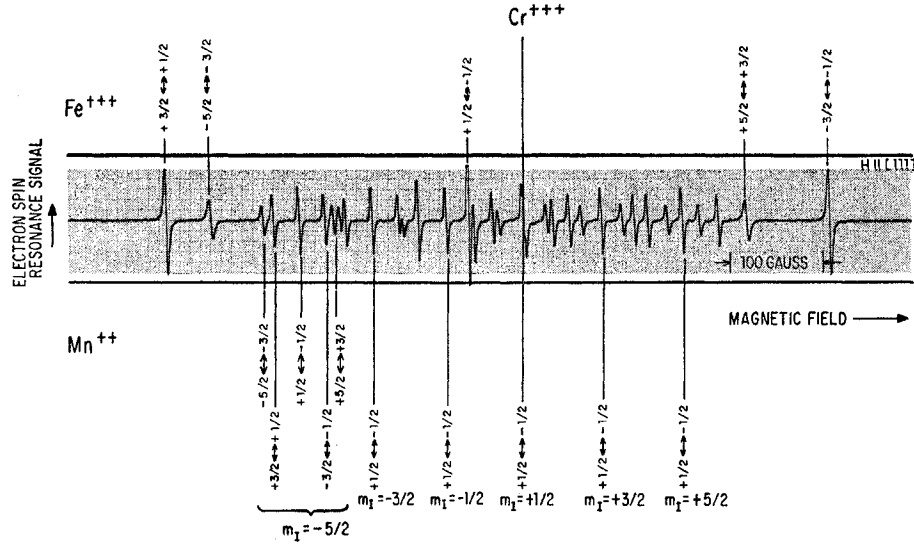
We can now express this D tensor as a linear function of the applied stresses or strains, in terms of constants of proportionality or spin-lattice coefficients. The linearity of the dependence is warranted by the smallness of the strains introduced (1 part in 10^4). It is also borne out experimentally, as shown in part B of this section. We write then $D_{ij}=\sum_{kl} C_{ijkl} X_{kl}$ where X_{kl} are the components of the external stresses. (In this case the spin-lattice coefficients C_{ijkl}, are called "stress coefficients." If D_{ij} is expressed in terms of strains, instead, then the constants of proportionality are denoted by G_{ijkl} and are called "strain coefficients.")

Shulman, Wyluda, and Anderson[5] point out that a relation such as we have written for D is of the same form as the generalized Hooke's law, and they show that the spin-lattice coefficients will obey similar relations to those that obtain between the elastic constants for crystals of cubic symmetry. Namely, in terms of the contracted Voigt notation, $C_{11}=C_{22}=C_{33}$; $C_{44}=C_{55}=C_{66}$; $C_{12}=C_{23}=C_{21}=C_{32}=C_{13}$. The tracelessness of D adds one further condition: $C_{11}=-2C_{12}$. We are therefore left with two independent constants, C_{11} and C_{44}. We write, then, for the relation between the components of D and the components of X:

$$\begin{bmatrix} D_{11} \\ D_{22} \\ D_{33} \\ D_{12} \\ D_{23} \\ D_{31} \end{bmatrix} = \begin{bmatrix} C_{11} & -\frac{1}{2}C_{11} & -\frac{1}{2}C_{11} & 0 & 0 & 0 \\ -\frac{1}{2}C_{11} & C_{11} & -\frac{1}{2}C_{11} & 0 & 0 & 0 \\ -\frac{1}{2}C_{11} & -\frac{1}{2}C_{11} & C_{11} & 0 & 0 & 0 \\ 0 & 0 & 0 & C_{44} & 0 & 0 \\ 0 & 0 & 0 & 0 & C_{44} & 0 \\ 0 & 0 & 0 & 0 & 0 & C_{44} \end{bmatrix} \begin{bmatrix} X_{11} \\ X_{22} \\ X_{33} \\ X_{12} \\ X_{23} \\ X_{31} \end{bmatrix}.$$

(1)

---

[5] R. G. Shulman, B. S. Wyluda, and P. W. Anderson, Phys. Rev. **107**, 953 (1951).

FIG. 2. Typical electron spin resonance spectrum of paramagnetic impurities in MgO, observed at 77°K and with $H\|[111]$ axis ($\nu_e \approx 10\,000$ Mc/sec). The complexity of the spectrum is due mainly to the thirty transitions of Mn²⁺. For the orientation shown, the Mn²⁺ lines are flanked at both ends of the spectrum by the Fe³⁺ fine structure; at other angles, the Fe²⁺ fine structure approaches the central transition near $g=2.00$ and so merges into the M²⁺ spectrum. A certain amount of Cr³⁺ is almost always present in these samples; its resonance signal is only partially resolved from the central, $m_I=+\frac{1}{2}$, Mn²⁺ line in the trace shown.

In terms of the components of the applied stress, then, $\mathfrak{K}_{nc}$ becomes

$$\mathfrak{K}_{nc}=C_{11}\{[X_{11}-\tfrac{1}{2}(X_{22}+X_{33})]S_1{}^2$$
$$+[X_{22}-\tfrac{1}{2}(X_{33}+X_{11})]S_2{}^2$$
$$+[X_{33}-\tfrac{1}{2}(X_{22}+X_{11})]S_3{}^3\}+C_{44}\{X_{12}(S_1S_2+S_2S_1)$$
$$+X_{13}(S_1S_3+S_3S_1)+X_{23}(S_2S_3+S_3S_2)\}\,.$$

Assuming, as indeed is the case experimentally, that $D\ll g\beta H$, we treat now $\mathfrak{K}_{nc}$ as a perturbation on $\mathfrak{K}_c$. In order to find the shift of the energy levels under stress, we diagonalize the Hamiltonian. We do this in the coordinate system where the Zeeman term has the simple form $g\beta HS_3{}'$. Calling φ and θ the polar angles of the magnetic field with respect to the cubic crystalline axes, we can write the components of the spin along the cubic crystalline axes in terms of the new components and evaluate the diagonal elements of the Hamiltonian. We get thus an expression for the shift, to first order, of the energy level characterized by the magnetic quantum number m_s. Correspondingly, the change under stress of the magnetic field at which the transition $m_s\to(m_s-1)$ appears, is given by

$$\delta H_{m_s\to m_s-1}=-(2m_s-1)\{\tfrac{3}{2}C_{11}[X_{11}(\tfrac{3}{2}\cos^2\varphi\sin^2\theta-\tfrac{1}{2})$$
$$+X_{22}(\tfrac{3}{2}\sin^2\varphi\sin^2\theta-\tfrac{1}{2})+X_{33}(\tfrac{3}{2}\cos^2\theta-\tfrac{1}{2})]$$
$$+3C_{44}[X_{12}\cos\varphi\sin\varphi\sin^2\theta+X_{23}\cos\theta\sin\theta\sin\varphi$$
$$+X_{31}\sin\theta\cos\theta\cos\varphi]\}\,. \quad (2)$$

This expression gives to first order the shift under stress of any transition for any angle (φ,θ) of the magnetic field with respect to the cubic axes of the crystal and for an external stress applied in any direction. The X_{ij} are the components of the applied stress in the cubic system of axes of the crystal; the C_{11} and C_{44} are the

constants defined by Eq. (1). We see then that

$$\delta H(m_s=+\tfrac{1}{2}\to-\tfrac{1}{2})=0,$$
$$\delta H(m_s=\pm\tfrac{3}{2}\to\pm\tfrac{1}{2})=\pm f(X_{ij},C_{ij},\varphi,\theta), \quad (3)$$
$$\delta H(m_s=\pm\tfrac{5}{2}\to\pm\tfrac{3}{2})=\pm2f(X_{ij},C_{ij},\varphi,\theta).$$

That is: to first order, the $+\tfrac{1}{2}\to-\tfrac{1}{2}$ transition remains unchanged, and the $\pm\tfrac{5}{2}\to\pm\tfrac{3}{2}$ transitions vary twice as much as the $\pm\tfrac{3}{2}\to\pm\tfrac{1}{2}$ for a given angle and external pressure.

It is customary to express the spin Hamiltonian of a noncubic crystal in terms of the constants D and E. In such a case the term $\sum_{ij}D_{ij}S_iS_j$ is expressed in components referred to the axes 1, 2, 3 of the deformation; D_{ij} is diagonal so $\mathfrak{K}_{nc}$ can be written $D_{11}S_1{}^2+D_{22}S_2{}^2+D_{33}S_3{}^2$ and calling

$$D=\tfrac{3}{2}D_{33}, \quad\text{and}\quad E=\tfrac{1}{2}(D_{11}-D_{22})$$

then

$$\mathfrak{K}_{nc}=D[S_3{}^2-\tfrac{1}{3}S(S+1)]+E[S_1{}^2-S_2{}^2]\,,$$

In terms now of the polar angles φ', θ' of the magnetic field with respect to the deformation axes:

$$\delta H_{m_s\to m_s-1}=-(2m_s-1)[D(\tfrac{3}{2}\cos^2\theta'-\tfrac{1}{2})$$
$$+\tfrac{3}{2}E\cos^2\varphi'\sin^2\theta']\,. \quad (4)$$

We now specialize Eqs. (2) and (4) to three useful cases (see Fig. 1), by giving explicitly the shifts of the $+\tfrac{3}{2}\to+\tfrac{1}{2}$ transition under an applied pressure P.

Case i. Pressure $P\|[001]$. The stress components along the cubic axes are: $X_{33}=P$; $X_{11}=X_{22}=X_{12}=X_{23}=X_{31}=0$.

$$f=-\tfrac{3}{2}C_{11}P(3\cos^2\theta-1)\,,$$
$$D=\tfrac{3}{2}C_{11}P \quad\text{and}\quad E=0\,.$$
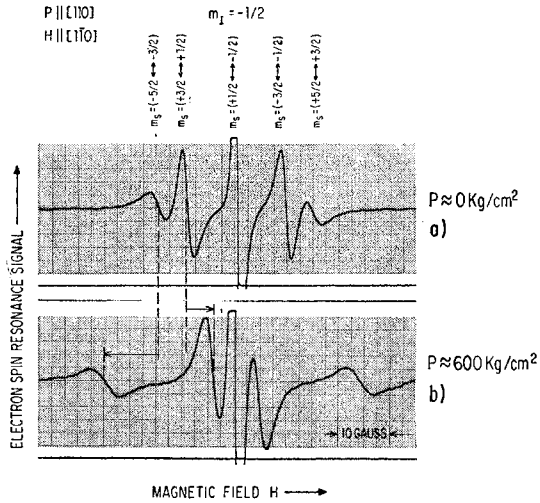
FIG. 3. Electron spin resonance signal of the $m_I = -\frac{1}{2}$ pentad of Mn^{2+}, observed with $H\|[1\bar{1}0]$ and $P\|[110]$ at 77°K. (a) shows and labels the electronic transitions in the absence of external stress. (b) shows the displacement of the transitions when $P \approx 600$ kg/cm²; the lines $m_s = -\frac{5}{2} \rightarrow -\frac{3}{2}$ and $m_s = -\frac{3}{2} \rightarrow -\frac{1}{2}$ shift to lower fields and the other two lines to higher magnetic fields. Also the $m_s = \pm\frac{5}{2} \rightarrow \pm\frac{3}{2}$ transitions shift more than the $m_s = \pm\frac{3}{2} \rightarrow \pm\frac{1}{2}$ lines.

Case ii. Pressure $P\|[110]$. The stress components along the cubic axes are: $X_{11} = X_{22} = X_{12} = \frac{1}{2}P$; $X_{13} = X_{23} = X_{33} = 0$.

$$f = -P\{\tfrac{3}{2}C_{11}(\tfrac{3}{2} \sin^2\theta - 1) + 3C_{44} \cos\varphi \sin\varphi \sin^2\theta\},$$

$$D = -\tfrac{3}{4}C_{11}P \quad \text{and} \quad E = \tfrac{1}{2}C_{44}P.$$

Case iii. Pressure $P\|[111]$. The stress components along the cubic axes are: $X_{11} = X_{22} = X_{33} = X_{12} = X_{23} = X_{31} = \frac{1}{3}P$.

$$f = -2C_{44}P\{\cos\varphi \sin\varphi \sin^2\theta + \cos\theta \sin\theta(\cos\varphi + \sin\varphi)\},$$

$$D = +C_{44}P \quad \text{and} \quad E = 0.$$

B. Experimental Results

Figure 2 shows the transitions observed in a typical spectrum of Mn^{2+} and Fe^{3+} in cubic MgO. Figures 3 and 4 indicate the nature of the changes observed in this spectrum when a uniaxial stress is applied.

a. The Effect of Uniaxial Stress on the Parameters A, g, and a

In the discussion of part A of this section, we have assumed that the only effect of a uniaxial stress is to introduce a deformation from cubic symmetry, leaving the cubic portion of the spin Hamiltonian (i.e., g, a, A) unchanged. We now examine the validity of this assumption which has been tested experimentally.

We have determined limits of variation for A and g of Mn^{2+} and g of Fe^{3+} at 77°K and under pressures up to ≈ 600 kg/cm². The observations were made with $P\|[110]$ and $H\|[001]$, and consisted in determining

the position of the central $H(m_s = +\frac{1}{2} \rightarrow -\frac{1}{2}; m_I = \pm\frac{5}{2})$ transitions, which we refer to below as $H_c(m_I)$ for the sake of brevity.

The expressions that give the field H at which the transitions appear in a cubic field, are given explicitly elsewhere.[2,3] From those expressions, a change in the cubic field parameters can be expressed so:

$$\left.\frac{\delta g}{g}\right|_{Mn^{2+}} = \frac{\delta H_c(+\frac{5}{2}) + \delta H_c(-\frac{5}{2})}{H_c(+\frac{5}{2}) + H_c(-\frac{5}{2})},$$

$$\left.\frac{\delta A}{A}\right|_{Mn^{2+}} = \frac{\delta H_c(+\frac{5}{2}) - \delta H_c(-\frac{5}{2})}{H_c(+\frac{5}{2}) - H_c(-\frac{5}{2})},$$

$$\delta g/g|_{Fe^{3+}} = \delta H_c/H_c.$$

No variation with pressure was observed in any of the three parameters, within the limits of experimental accuracy. [These limits are given by the limits in the reproducibility of the center of a given line $H_c(m_I)$ rather than by the actual determination of such a center.]

Thus, $\delta g/g|_{Mn^{2+}} \leq 0.001\%$; $\delta A/A|_{Mn^{2+}} \leq 0.01\%$ and $\delta g/g|_{Fe^{3+}} \leq 0.003\%$.

In order to test experimentally for the lack of change in a we now focus our attention on the fine structure transitions, which are the ones that would show such a change to first order. We assume the change δa introduced by an external stress is small and so neglect
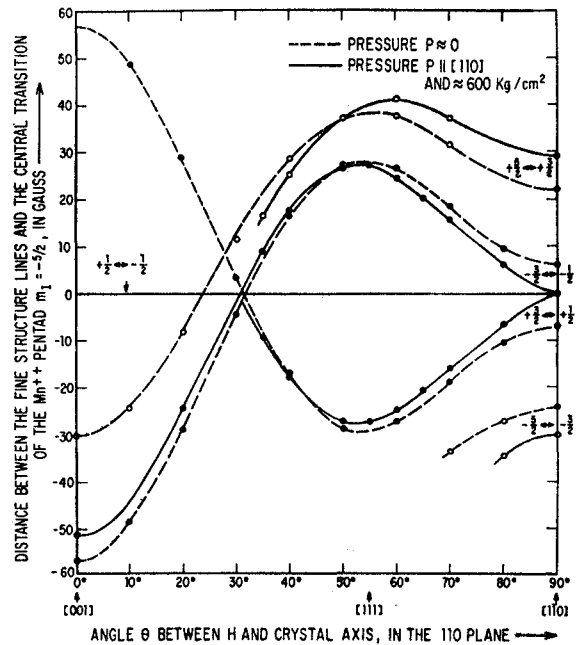

FIG. 4. Plot of the distance in gauss between the fine structure lines and the central $+\frac{1}{2} \rightarrow -\frac{1}{2}$ transition of the Mn^{2+} pentad $m_I = -\frac{5}{2}$, as a function of the direction of the magnetic field in the (110) plane. The dashed lines show the angular dependence in the absence of external pressure; the full lines show the angular dependence with $P\|[110]$ and $P = 580$ kg/cm².
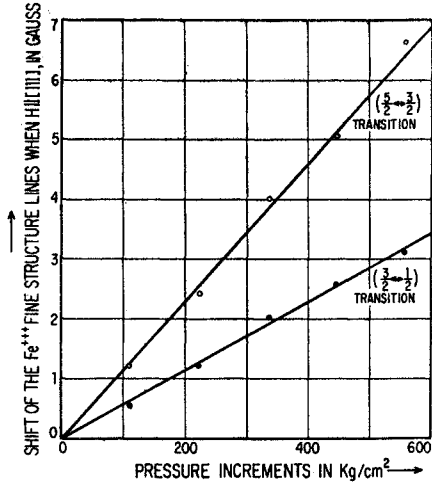
FIG. 5. Plot of the absolute magnitude of the shift of the fine structure resonance lines of Fe^{3+} versus increments of applied pressure. These data were taken with $H\|[111]$ and $P\|[1\bar{1}0]$ at 77°K. The plot shows the linearity of the shifts with applied pressure; it also shows that the $m_s = \pm\frac{5}{2} \to \pm\frac{3}{2}$ transitions are displaced twice as much as the $m_s = \pm\frac{3}{2} \to \pm\frac{1}{2}$ transitions, for a given applied pressure.

second-order terms in a. Then the change in field δH at which the fine structure transitions appear gives the ratio

$$\frac{\delta H(m_s = \pm\frac{5}{2} \to \pm\frac{3}{2})}{\delta H(m_s = \pm\frac{3}{2} \to \pm\frac{1}{2})} = \frac{\mp 2p\delta a}{\pm\frac{5}{2}p\delta a} = -\frac{4}{5}.$$

However, the ratio observed experimentally is $+2.03 \pm 0.03$. The sign of this ratio is apparent from Fig. 3, where we show the effect of an applied external pressure on a spin pentad (that of Mn^{2+}, $m_I = -\frac{1}{2}$). The magnitude of the ratio is obtained from plots like the one presented in Fig. 5, which shows for Fe^{3+} and $H\|[111]$, the absolute magnitude of the shift versus pressure of both the $\frac{5}{2} \to \frac{3}{2}$ and the $\frac{3}{2} \to \frac{1}{2}$ transitions. Similar plots are obtained for different orientations of the magnetic field and for Mn^{2+}.

We therefore see that the magnitude and sign of the shifts of the resonance lines observed are consistent with a description of the system with a term in D_{ij} being introduced into the spin Hamiltonian, but inconsistent with a change in a. (In terms of our experimental errors, if such a change is present, it must be smaller than 1% of the D term introduced.)

b. The Parameters D, E, and the Determination of C_{11} and C_{44}

The term D_{ij} is related to the external stress by the constants C_{11} and C_{44}. These constants can be obtained directly from two distinct axially symmetric distortions of the sample obtained, respectively, by stressing along the [001] and along the [111] axes (cf. cases i and iii, Sec. IIA). For this, however, it is necessary to use two different samples, and experimentally it is desirable to

be able to determine both constants in the same sample and during the same run. This is possible if we do not introduce an axially symmetric distortion but a more complicated one corresponding to case ii, discussed previously. This is the procedure we have adopted.

Samples were cut with edges parallel to the [001], [110], and [1$\bar{1}$0] axes and the external stress was applied along the [110] axis. Then, observation of the displacement of a transition along two different directions gives enough information to obtain both C_{11} and C_{44}. Two convenient directions are $H\|[001]$ and $H\|[111]$, since in these cases we can obtain C_{11} and C_{44} separately. However, the direction $H\|[111]$ is very sensitive to any misorientations in the system (see Appendix). Therefore, from considerations of accuracy it is more desirable to determine C_{44} from the shifts observed with $H\|[1\bar{1}0]$. This is, indeed, what we have done in the case of Mn^{2+}. For Fe^{3+}, however, it was not possible to resolve the fine structure along the [1$\bar{1}$0] since it broadens (see Sec. III) and merges into the Mn^{2+} spectrum. For Fe^{3+}, then, C_{44} was determined with $H\|[111]$.

The determination of the constants C_{ij} was made by comparing at various pressures the difference in the magnetic fields at which appear a given fine structure line and the central $+\frac{1}{2} \to -\frac{1}{2}$ transition of its pentad (i.e., of the same m_I in the case of Mn^{2+}). From Eq. (3)

$$[H(\pm\tfrac{5}{2} \to \pm\tfrac{3}{2}) - H(+\tfrac{1}{2} \to -\tfrac{1}{2})]_{\text{stress}P}$$
$$- [H(\pm\tfrac{5}{2} \to \pm\tfrac{3}{2}) - H(+\tfrac{1}{2} \to -\tfrac{1}{2})]_{\text{zero stress}}$$
$$= \pm 2f(X_{ij}, C_{ij}, \varphi, \theta)$$

and

$$[H(\pm\tfrac{3}{2} \to \pm\tfrac{1}{2}) - H(+\tfrac{1}{2} \to -\tfrac{1}{2})]_{\text{stress}P}$$
$$- [H(\pm\tfrac{3}{2} \to \pm\tfrac{1}{2}) - H(+\tfrac{1}{2} \to -\tfrac{1}{2})]_{\text{zero stress}}$$
$$= \pm f(X_{ij}, C_{ij}, \varphi, \theta).$$

In practice, in our experimental setup, the state of zero stress is not well defined mechanically. It is necessary to keep the system always under a small amount of pressure so that the two halves of the resonant cavity and hence the crystalline sample remain in place and aligned. We make use then of the linear dependence of f on P and normalize the shifts not to zero pressure but to some initial pressure P' ($P' \approx 100$ kg/cm² in our experiments). Thus, for instance,

$$f = [H(+\tfrac{3}{2} \to +\tfrac{1}{2}) - H(+\tfrac{1}{2} \to -\tfrac{1}{2})]_{\text{stress}(P+P')}$$
$$- [H(+\tfrac{3}{2} \to +\tfrac{1}{2}) - H(+\tfrac{1}{2} \to -\tfrac{1}{2})]_{\text{stress}P'},$$

and from case ii Sec. IIA:

if $H\|[001]$ then $f = -2D = +\tfrac{3}{2}PC_{11}$;

if $H\|[111]$ then $f = +2E = +PC_{44}$;

if $H\|[1\bar{1}0]$ then $f = +(D-3E) = -3P(\tfrac{1}{4}C_{11} - \tfrac{1}{2}C_{44})$.

Table I shows the experimental values obtained for the stress coefficients. The absolute values of the constants are obtained from the plots of Figs. 6 and 7.

TABLE I. The experimentally determined stress coefficients
in units of 10^{-13} cm/dyne.

	Mn^{2+}	Fe^{3+}
C_{11}	$+7.1$	$+26$
C_{44}	-2.1	-5.5

Their signs are obtained by observing the displacement
under stress of the lines that form a spin pentad (Fig. 3).

The experimental errors are $\pm 3\%$ with the exception
of C_{44} for Fe^{3+} where it is $\pm 6\%$. A discussion of the
origin of these experimental errors and their estimate is
given in the Appendix.

Since C_{44} and C_{11} for any one ion have been deter-
mined at the same pressure, their ratio is known to a bet-
ter accuracy than the absolute values, namely 2% for
Mn^{2+} and 5% for Fe^{3+}.

It must be emphasized that these constants are
evaluated from a first-order perturbation theory. In
point of fact, a in Fe^{3+} is large enough so that when we
neglect second-order terms of the form (Da/H_0) in
our energy level expressions, we are making an error
of the same order as the experimental errors. In our
experimental results we see the deviations due to these
second-order terms. While for Mn^{2+} the experimental
points due to the transitions $+(m_s \rightarrow m_s-1)$ and
$-(m_s \rightarrow m_s-1)$ fall in the same straight line within
our error, in the case of Fe^{3+} there is a net difference
which is proportional to pressure. In order to reduce the
errors arising from the neglect of second-order terms,
the values we have plotted in Fig. 6 and from which we
have obtained the C_{ij}'s are the arithmetical average of
the $\pm\frac{3}{2} \rightarrow \pm\frac{1}{2}$ shifts.

Similar experiments to the ones described were in-
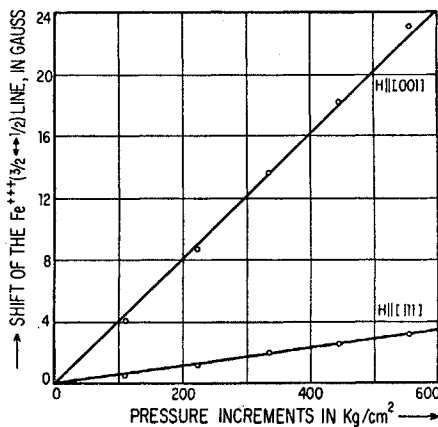dependently carried out by Watkins. His values and our

FIG. 6. Plot of the absolute magnitude of the average of the
shifts of the $m_s = \pm\frac{3}{2} \rightarrow \pm\frac{1}{2}$ transitions of Fe^{3+} versus increments
of applied pressure. Zero shift corresponds to the position of the
lines under an external pressure of 111 kg/cm². The data were
taken at 77°K and with $P\|[110]$. The slope of the line labeled
$H\|[001]$ is given by $|\frac{3}{2}C_{11}|$; the line labeled $H\|[111]$ has a
slope $= \lceil C_{44} \rceil$. Hence, $|C_{11}| = 2.6 \times 10^{-13}$ cm/dyne and $|C_{44}|$
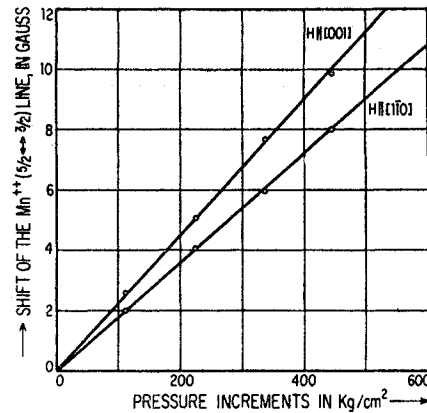$= 5.5 \times 10^{-13}$ cm/dyne are obtained from this plot.

FIG. 7. Plot of the absolute magnitude of the shift of the
$m_s = -\frac{1}{2} \rightarrow -\frac{3}{2}$ transition of Mn^{2+} $(m_I = \frac{5}{2})$ versus increments of
applied pressure. Zero shift corresponds to the position of the lines
under an external pressure of 222 kg/cm². The data were taken
at 77°K and with $P\|[110]$. The slope of the line labeled
$H\|[001]$ is given by $|\frac{3}{2}C_{11}|$; the line labeled $H\|[110]$ has a
slope $= \lceil 3(\frac{1}{2}C_{11}-\frac{1}{4})C_{44} \rceil$. Hence, $|C_{11}| = 7.1 \times 10^{-13}$ cm/dyne and
$|C_{44}| = 2.1 \times 10^{-13}$ cm/dyne are obtained from this plot.

preliminary ones agreed well within the experimental
errors, and were published together in unified form.[6] The
numbers published then were the strain coefficients G_{ij}.
Throughout this work, however, we have used the stress
coefficients C_{ij} because we feel they have greater physi-
cal significance in our experiments since we measure
stresses rather than strains. To express our results in
terms of G_{ij} it is necessary to use the elastic coefficients
of MgO. Thus, in terms of the elastic stiffnesses c_{ij}:

$$G_{11}/(c_{11}-c_{12})=C_{11} \quad \text{and} \quad G_{44}/c_{44}=C_{44},$$

where[7]

$$c_{11}=29.54\times 10^{11} \text{ dyn/cm}^2; \quad c_{12}=8.49\times 10^{11} \text{ dyn/cm}^2;$$

$$c_{44}=14.99\times 10^{11} \text{ dyn/cm}^2.$$

Germanier, Gainon, and Lacroix[8] have also deter-
mined the D term of Fe^{3+} and Mn^{2+} in an MgO sample
that is stressed uniaxially along a cubic crystalline axis.
In our terminology their results are:

$$C_{11}(Mn^{2+})=(12\pm 2)\times 10^{-13} \text{ cm/dyn}$$

and

$$C_{11}(Fe^{3+})=(37\pm 4)\times 10^{-13} \text{ cm/dyn}.$$

A later revision of their results[9] yielded $C_{11}(Mn^{2+})$
$=8.8\times 10^{-13}$ cm/dyn and $C_{11}(Fe^{3+})=31\times 10^{-13}$ cm/
dyn. These results are still large, and agree with ours
only marginally within the experimental limits.

[6] G. Watkins and Elsa Feher, Bull. Am. Phys. Soc. 7, 29 (1962).
[7] A. L. Schawlow, A. H. Piksis, and S. Sugano, Phys. Rev. 122, 1469 (1961).
[8] A. M. Germainier, D. Gainon, and R. Lacroix, Phys. Letters 2, 105 (1962).
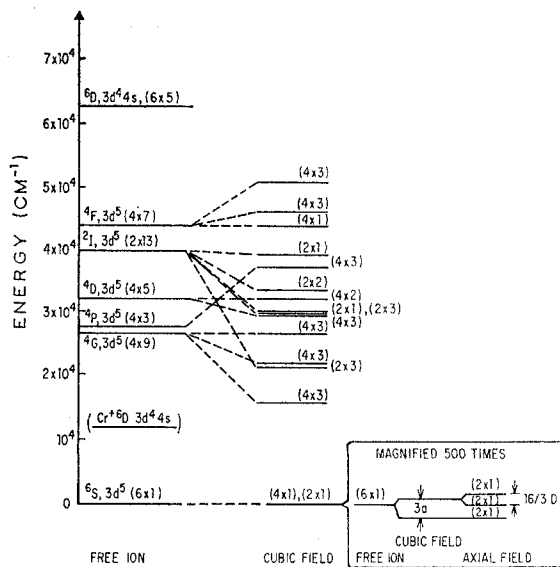[9] R. Lacroix (private communication).

FIG. 8. Diagram showing the lowest lying energy levels of the free Mn^{2+} and how they split in a cubic crystalline field [see Refs. 11 and L. E. Orgel, J. Chem. Phys. **23**, 1004 (1955); Y. Tanabe and S. Sugano, J. Phys. Soc. Japan **9**, 766 (1954); C. Moore, Natl. Bur. Std. (U. S.) Circ. No. 467 (1962)] of strength approximately that of MgO [$Dq \approx 1250$ cm^{-1} (see T. R. Gabriel, D. F. Johnson, and M. T. Powell, Proc. Roy. Soc. (London) **263A**, 503 (1961))]. For reference we show the lowest lying state ^6D of the first excited configuration $3d^44s$ of Cr$^+$. The numbers in parentheses give the total degeneracy of a state: spin degeneracy times orbital degeneracy. The splitting of the ground state ^6S is magnified in the insert. The insert shows to scale how the sixfold degenerate state splits in a cubic and pressure induced axial field ($P \approx 500$ kg/cm^2) into a Kramers triplet.

c. Comparison of Experiment with Theory

There have been many attempts to obtain the D_{ij} from first principles. One of the difficulties of such calculations, is that the ground state of the ions Mn^{2+} and Fe^{3+} is an orbital singlet. Now, the electron spins can only be affected by the electric crystalline field of the lattice through their orbital angular momentum. Therefore, there will be a spin-lattice interaction only insofar as the ground state is not a pure S state but has admixed into it some higher lying energy states with nonvanishing angular momentum. The problem then is: what are the mechanisms that admix these excited states?

Pryce[10] proposed that the important mechanism is a second-order process involving the axial field V_{ax} and the spin-spin coupling V_{ss}, via an intermediate state (see Fig. 8) from an excited configuration.

Watanabe[11] added another mechanism to the above: a fourth-order process, quadratic in the axial field and in the spin-orbit interaction. He made an explicit calculation for Mn, of $D = D$(Watanabe)$+ D$(Pryce)$= -A\Delta^2 + B\Delta$. Expressing D in cm^{-1}, the constants A and B are approximately 10^{-9} and 10^{-6}, respectively. The param-

eter Δ is a measure of the strength of the axial crystalline field ($V_{ax} = c_{20}r^2Y_0{}^2$, expressing V_{ax} in spherical harmonics $Y_n{}^m$ and $\Delta = \frac{1}{4}(5\pi^{-1})^{1/2}c_{20}\langle r^2 \rangle$ as defined by Watanabe). The usual axial fields are of order $\Delta = 10^{+3}$ cm^{-1}, and both the linear and quadratic terms contribute to D. However, for our stress experiments a point-charge calculation shows that at the pressures we use, the axial fields introduced are $\Delta \approx 10$ cm^{-1}. The term quadratic in the axial field then drops out and only Pryce's mechanism remains operative. The D values obtained for Mn^{2+} using Watanabe's calculation of Pryce's mechanism are approximately one order of magnitude less than those found experimentally. There is a certain amount of indeterminacy in these estimates because they involve the overlap of the radial wave functions of the $3d$ and $4s$ electrons which is not well known.

Germanier, Gainon, and Lacroix[8] also tried to obtain a theoretical interpretation of the D terms. They considered, in addition to Pryce's mechanism, two other processes that contribute to the part of D that is linear in V_{ax}. Their result, however, is 100 times too small and also of the wrong sign.

Blume and Orbach[12] have obtained the strain coefficients of Mn^{2+} in MgO through a refined calculation that takes into account the spin-orbit coupling and the axial crystalline field. Thus they obtain for Mn^{2+} in MgO, $G_{11} = -1.21$ cm^{-1}/unit strain ($\therefore C_{11} = -5.7 \times 10^{-13}$ cm/dyn); and $G_{44} = +0.0391$ cm^{-1}/unit strain ($\therefore C_{44} = +0.26 \times 10^{-13}$ cm/dyn), a result that is of the wrong sign compared with experiment (cf. Table I). The authors feel that the difficulty lies in the use of a point-charge model to evaluate constants. An alternate explanation would be that their assumed mechanism is not the only one present.

A refined version of the process of Pryce, introducing spin-spin coupling in the presence of an axial field, was worked out by Leushin,[13] who obtained $G_{11} = +0.52$ cm^{-1}/unit strain ($\therefore C_{11} = +2.5 \times 10^{-13}$ cm/dyn) and $G_{44} = -0.37$ cm^{-1}/unit strain ($\therefore C_{44} = -2.5 \times 10^{-13}$ cm/dyn). This result is of the right sign compared with experiment; it is also of the right order of magnitude although, once again, there is a certain amount of indeterminacy due to the fact that the overlap of the $3d$ and $4s$ electronic wave functions is not well known.

A different approach to the same problem is presented by Kondo.[14] He argues that all efforts so far have been based on naïve crystalline theories which take into account the deformation of the metal ion by mixing in higher excited states by the crystalline field, but where no attention is paid to overlap and covalency. By taking these into account, Kondo obtains the spin-lattice coefficients in terms of two parameters which he can fit

[10] M. H. L. Pryce, Phys. Rev. **80**, 1107 (1950).
[11] H. Watanabe, Progr. Theoret. Phys. (Kyoto) **18**, 405 (1957).

[12] M. Blume and R. Orbach, Phys. Rev. **127**, 1587 (1962).
[13] A. M. Leushin, Fiz. Tverd. Tela. **5**, 605 (1963) [English transl.: Soviet Phys.–Solid State **5**, 440 (1963)]. I wish to thank Dr. R. Orbach for having brought this work to my attention.
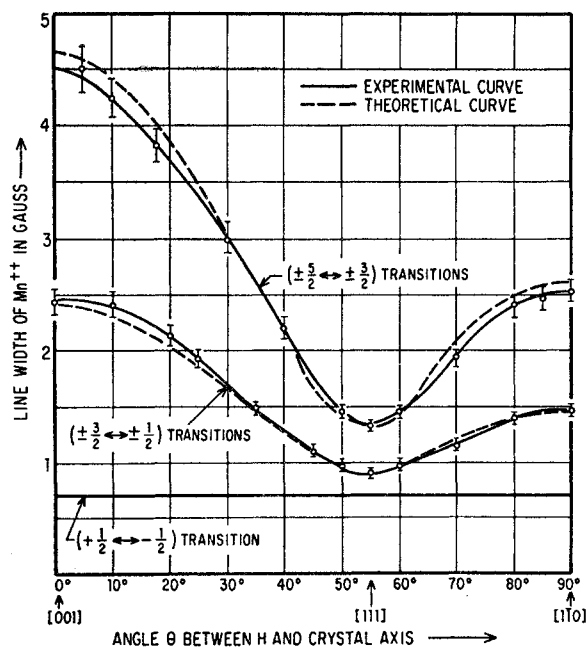[14] J. Kondo, Progr. Theoret. Phys. (Kyoto) **28**, 1026 (1962).

FIG. 9. Linewidth of the fine structure of Mn^{2+} ($m_I = -\frac{5}{2}$) as a function of the direction of the magnetic field in the (110) plane; $T = 77°K$. The theoretical curve is a plot of Eq. (6) with $\alpha = 104$ kg/cm^2 and $\beta = 96$ kg/cm^2.

so that G_{11} and G_{44} agree with our experimentally observed values.
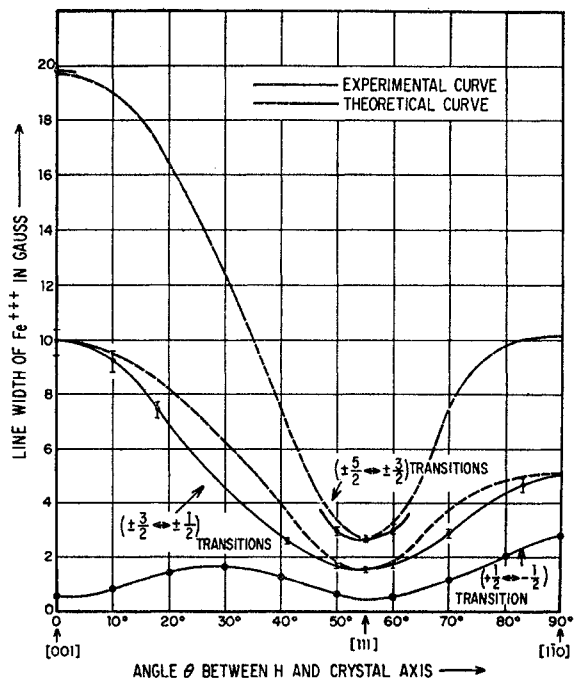
Probably all three mechanisms proposed contribute

FIG. 10. Linewidth of Fe^{3+} as a function of the direction of the magnetic field in the (110) plane; $T = 77°K$. The theoretical curve is a plot of Eq. (6) with $\alpha = 112$ kg/cm^2 and $\beta = 80$ kg/cm^2.

to the constants G_{11} and G_{44}: spin-orbit mixing of higher excited states, spin-spin mixing of higher excited configurations, and overlap and covalency. We do not know, however, what their relative importance is and a good theoretical account of the origin and magnitude of the spin-lattice coefficients is yet wanting.

This lack of satisfactory agreement between experimental and theoretical spin-lattice coefficients manifests itself also in the evaluation of direct spin-lattice relaxation times. Blume and Orbach, and also Kondo, in the papers referred to above, calculate T_1 for Mn^{2+} in MgO. They both obtain expressions for T_1 in terms of G_{11} and G_{44}, which, evaluated with our experimentally determined spin-lattice coefficients yield relaxation times that roughly agree with preliminary measurements of Castle and Feldman[15] of the direct process. This seems to indicate that even though efforts to calculate T_1 must fail if the spin-lattice coefficients cannot be
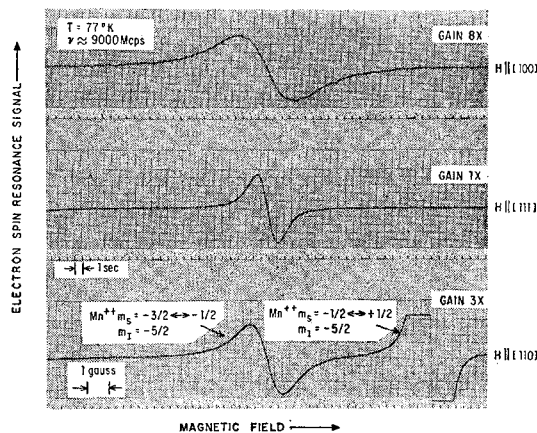

FIG. 11. Change in width of the electron spin resonance line observed for three different directions of the magnetic field; $T = 77°K$ and $\nu \approx 9000$ Mc/sec. The traces depict the Mn^{2+} transition, $m_s = -\frac{3}{2} \rightarrow -\frac{1}{2}$, $m_I = -\frac{5}{2}$, but all of the fine structure lines of Mn^{2+} or Fe^{3+} show a similar behavior.

accounted for theoretically, it is still possible to obtain T_1 in terms of the experimentally obtained spin-lattice coefficients used as phenomenological parameters.

III. LINEWIDTHS OF Mn^{2+} AND Fe^{3+} IN MgO

A. The Fine Structure Lines

a. The Observed Linewidths and Their Presumed Origin

We have plotted in Figs. 9 and 10 the angular dependence of the linewidths of the Mn^{2+} and Fe^{3+} transitions as observed in the (110) plane at 77°K. The outstanding feature of these curves is that the linewidths are largest with $H\|[001]$ and least with $H\|[111]$ (see also Fig. 11). In the present section we will show that this variation in linewidth is due to stresses built into

---

[15] J. G. Castle and D. Feldman (unpublished).

the crystal, and we will account for it quantitatively by assuming a random distribution of internal stresses.[16]

From Eq. (2) it can be seen that the shifts of the resonance lines observed with $H\|[001]$ are proportional to C_{11} only, while the shifts observed with $H\|[111]$ are proportional to C_{44} only. Since for Mn^{2+} and Fe^{3+} $|C_{11}|>C_{44}|$, it seems likely that a random distribution of internal stresses in the crystal will give rise to linewidths that vary with angle as those observed. This supposition is strongly substantiated by observing the linewidths along the cubic axes, where the effect of stress is most pronounced. From the experimental curves, with $H\|[001]$ we note that the ratio of the linewidths:

$$\frac{\Delta H \text{ of the } (\pm\tfrac{5}{2} \to \pm\tfrac{3}{2}) \text{ transition}}{\Delta H \text{ of the } (\pm\tfrac{3}{2} \to \pm\tfrac{1}{2}) \text{ transition}} = \text{the ratio}$$

of the corresponding shifts under stress $= 2$.

Also with $H\|[001]$,

$$\frac{\Delta H \text{ of a fine structure transition in } Fe^{3+}}{\Delta H \text{ of the same fine structure transition in } Mn^{2+}}$$

$$= \frac{C_{11} \text{ in } Fe^{3+}}{C_{11} \text{ in } Mn^{2+}} \approx 4.$$

However, these ratios cease to hold as we leave the cubic axis and move toward the [111], where stresses are less effective and therefore, other broadening mechanisms may predominate. This leads us to the following assumption; the observed linewidth ΔH_{obs} of the fine structure is a superposition of two linewidths, one is that due to random internal stresses, which we call ΔH_S; the other is the intrinsic breadth ΔH_i which the line would have in the absence of internal stresses (i.e., $\Delta H_S = 0$) and which we take to be independent of m_s and of m_I. We assume, therefore,

$$\Delta H_{\text{obs}} = (\Delta H_S^2 + \Delta H_i^2)^{1/2}. \qquad (5)$$

b. Calculation of Linewidth Due to Stress

We assume that the total probability of the system being in a certain state of stress is given by the product of the probabilities of each of the components of the stress tensor, namely,

$$P_{\text{total}} = P(X_{12})P(X_{23})P(X_{31})P(X_{11})P(X_{22})P(X_{33}).$$

[16] Other workers in the field [i.e., J. W. Orton, P. Auzins, J. H. E. Griffiths, and J. E. Wertz, Proc. Phys. Soc. (London) 78B, 554 (1961); J. S. van Wieringen and J. G. Rensen, *Proceedings of the First International Conference on Paramagnetic Resonance, Jerusalem, 1962* (Academic Press Inc., New York, 1963), p. 105; N. S. Shiren, *ibid.*, p. 482; W. Low and J. T. Suss, Solid State Commun. 2, 1 (1964)] have considered that a distribution of lattice imperfections causes the linewidth of paramagnetic ions in MgO. However where quantitative estimates were attempted, the anisotropies were not properly taken into account. In any event, in the absence of the experimentally determined values of C_{11} and C_{44}, it is not possible to make any meaningful comparison between theory and experiment.

That is to say, we assume that the probabilities of the components of the stress tensor are uncorrelated. As to the form of these probabilities, calling X_{ij} the components of stress along the cubic axes of the system, we assume that the probability $P(X_{ij})$ of finding a stress component X_{ij} along the cubic axes is given by a Gaussian curve whose width is taken as a parameter to be fitted from the experimental values. We further assume that there are only two such parameters, i.e., that

$$P(X_{11}) = P(X_{22}) = P(X_{33}) = P(X_{ii})$$
$$= (2\pi^{-1})^{1/2}\alpha^{-1}\exp(-2X_{ii}^2/\alpha^2),$$

$$P(X_{12}) = P(X_{13}) = P(X_{23}) = P(X_{ij})$$
$$= (2\pi^{-1})^{1/2}\beta^{-1}\exp(2X_{ij}^2/\beta^2).$$

This is substantiated by the fact that the observed linewidths are identical when H lies along each of the three cubic crystal axes: [001], [010], [100]. Also the linewidths observed with H along the four-body diagonals: [111], [$\bar{1}$11], [1$\bar{1}$1], [11$\bar{1}$] should be the same (this is assumed but unchecked experimentally). With these assumptions we are now in a position to evaluate the second moment $\langle \delta H^2 \rangle$ of the observed resonance line:

$$\langle \delta H^2 \rangle = \int\int\int\int\int\int_{-\infty}^{+\infty} \delta H^2$$

$$\times \{\exp[-2(X_{11}^2 + X_{22}^2 + X_{33}^2)/\alpha^2]\}$$

$$\times \{\exp[-2(X_{12}^2 + X_{23}^2 + X_{13})/\beta^2]\}$$

$$\times (2/\pi\alpha\beta)^3 dX_{11}dX_{22}dX_{33}dX_{12}X_{13}dX_{23}.$$

Here δH^2 is obtained by squaring Eq. (2). Evaluating, we obtain[17]

$$\langle \delta H^2 \rangle_{m_s \to m_s-1} = (2m_{s-1})^2$$

$$\times \tfrac{3}{4}\left\{(C_{11}\tfrac{3}{2})^2\left(\frac{\alpha}{2}\right)^2(1-3F) + C_{44}^2\beta^2 3F\right\}$$

with

$$F = (\sin^2\theta\cos^2\theta + \sin^2\varphi\cos^2\varphi\sin^4\theta). \qquad (6)$$

For $\varphi = 45°$, i.e., for H lying in the (110) plane, this expression shows that

if $H\|[001]$, then $\langle \delta H^2 \rangle = (2m_s-1)^2(27/8)\alpha^2 C_{11}^2$;

if $H\|[111]$, then $\langle \delta H^2 \rangle = (2m_s-1)^2 3\beta^2 C_{44}^2$;

if $H\|[1\bar{1}0]$, then $\langle \delta H^2 \rangle = (2m_s-1)^2$
$$\times 3\{(9/32)\alpha^2 C_{11}^2 + \tfrac{3}{4}\beta^2 C_{44}^2\}. \qquad (7)$$

Equation (6) gives the linewidth of *any* transition for *any* angle (φ,θ) of the magnetic field with respect to the cubic axes of the crystal, in terms of two parameters α and β that characterize the distribution of internal stresses in the crystal. If both the crystal and the distribution of stresses were isotropic (this is *not* our case),

[17] Elsa Feher and M. Weger, Bull. Am. Phys. Soc. 7, 613 (1962).

the linewidth would be independent of angle and characterized by one parameter and one stress coefficient only.

c. Comparison of Experiment with Theory

In order to compare experiment with theory, we use now the symbol ΔH to denote the width of a line taken between the points of maximum slope. Since in our experiments we observe the derivative of the line, the quantity ΔH is what we directly measure. To express the predicted width in terms of ΔH we must just note that for a Gaussian line shape $\Delta H^2 = 4\langle\delta H^2\rangle$. Now, ΔH_S is proportional to $(2m_s - 1)$ [from Eq. (6)], so we can set

$$\Delta H_S(\pm\tfrac{5}{2} \to \pm\tfrac{3}{2}) = 2\Delta H_S(\pm\tfrac{3}{2} \to \pm\tfrac{1}{2}) \equiv 2\Delta H_S$$

throughout. From Eq. (5) then we obtain for the linewidth due to stress and for the intrinsic linewidth, respectively:

$$\Delta H_S{}^2 = \tfrac{1}{3}[\Delta H_{obs}{}^2(\pm\tfrac{5}{2} \to \pm\tfrac{3}{2})$$
$$- \Delta H_{obs}{}^2(\pm\tfrac{3}{2} \to \pm\tfrac{1}{2})], \quad (8)$$

and

$$\Delta H_i{}^2 = \Delta H_{obs}{}^2(\pm\tfrac{3}{2} \to \pm\tfrac{1}{2}) - \Delta H_S{}^2. \quad (9)$$

From the experimentally observed linewidth with $H\|[001]$ and Eqs. (7), (8), and (9), we obtain a value for α. Similarly, from the experimentally observed linewidth with $H\|[111]$ and Eqs. (7), (8), and (9), we obtain a value for β.

Evaluation of α and β for Mn^{2+}. From Eqs. (8) and (9) evaluated in the [111] direction, we obtain $\Delta H_i = 0.70$ G. This value of ΔH_i coincides with the linewidth of the central $(+\tfrac{1}{2} \to -\tfrac{1}{2})$ line, as expected, since the latter is unaffected by stresses to first order. We take ΔH_i to be independent of angle as the linewidth of the central line is independent of angle to first order. With this value of ΔH_i we now obtain ΔH_S in any direction from Eq. (9) using the appropriate observed value ΔH_{obs}. Comparing the ΔH_S obtained from Eq. (9) with that from Eq. (7) if $H\|[111]$, we obtain $\beta = 96$ kg/cm². Similarly, if $H\|[001]$ we obtain $\alpha = 104$ kg/cm². This is the arithmetic mean of the values of α obtained with $\Delta H_{obs}(\tfrac{5}{2} \to \tfrac{3}{2})$ and with $H_{obs}(\tfrac{3}{2} \to \tfrac{1}{2})$.

With these values of α and β we have plotted Eq. (6) in Fig. 9. It can be seen that the theoretical fit to the experimental curve is excellent. Whatever lack of agreement remains between the theoretical and experimental curves is probably due to the fact that the observed lines are not truly Gaussian as the theory assumes, but more nearly Lorentzian.

Evaluation of α and β for Fe^{3+}. Following a procedure analogous to that described for Mn^{2+}, we evaluate Eqs. (8) and (9) in the [111] and obtain $\Delta H_i = 0.84$ G. Taking this value to be independent of angle, we evaluate ΔH_S from Eq. (9) and hence α and β from Eq. (7). We obtain $\alpha = 112$ kg/cm² and $\beta = 80$ kg/cm². Equation (6) with these values of α and β has been plotted in Fig. 10.

The agreement with the experimental curve is not as good as for Mn^{2+}. This is not too surprising since the value found and used for ΔH_i does not portray the behavior of the central line at all. We see from Fig. 10 that the observed linewidth of the central Fe^{3+} line shows a marked angular dependence. If we assume ΔH_i to be a function of angle and to coincide at each point with the observed linewidth of the $Fe(+\tfrac{1}{2} \to -\tfrac{1}{2})$ line, then the theoretical curve obtained fits the experimental points very poorly.

Until we understand the mechanisms that broaden the central Fe^{3+} line (cf. Sec. IIIB) and how they, in turn, affect the fine structure, we cannot expect better agreement between theory and experiment than has been obtained.

d. Discussion of the Results

The error estimated in the determination of the experimental linewidths is $\pm 4\%$ which brings the error in α and β to $\pm 19\%$. The values of α and β obtained for Mn^{2+} and Fe^{3+} agree well within this margin. This was to be expected since the measurements reported were made on Fe^{3+} and Mn^{3+} in the same MgO sample.

We may conclude, then, that there remains no doubt that the dominant broadening of the fine structure lines of Mn^{2+} and Fe^{3+} in MgO is caused by stresses built into the crystal. Now that the line-broadening mechanism is understood and substantiated by experiment, it is possible to turn the problem around. Thus, the experimentally determined linewidths can be used to determine *quantitatively* the state of internal stress of a crystalline sample of MgO.

B. The Central (or $+\tfrac{1}{2} \to -\tfrac{1}{2}$) Transitions

The observed $(+\tfrac{1}{2} \to -\tfrac{1}{2})$ transitions are Lorentzian in shape. For Mn^{2+} the observed linewidth is ≈ 0.5 G. For Fe^{3+} the observed linewidth ranges approximately from 0.5–5 G, depending on temperature and angle. This striking behavior of the Fe^{3+} central line is depicted in Fig. 12.

Since these transitions are unaffected to first order by externally applied stress we would expect their linewidths to be equal to what we have termed the intrinsic linewidth ΔH_i. The question then arises: What is the origin of ΔH_i? The mechanisms that first come to mind are static dipolar broadening and broadening due to second-order stress effects. But these are too small in magnitude and would not give the observed angle and temperature dependence.

We are here confronted, then, with some gross unexplained effects. To name a few: the anisotropic linewidth; the relative magnitude of the linewidths at different temperatures; the fact that the broadening behavior is not the same for Mn^{2+} and Fe^{3+}. Much more experimental and theoretical work will be necessary to understand the processes that occur and give rise to these features.
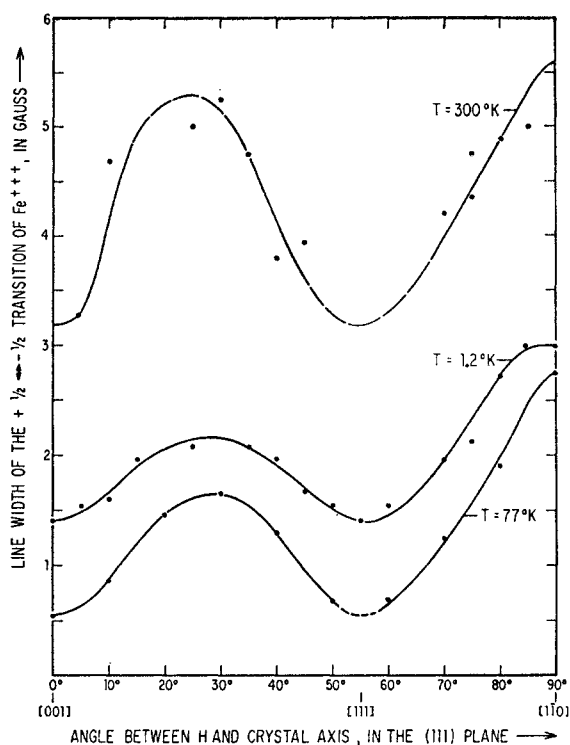
FIG. 12. Observed linewidth of the $+\frac{1}{2} \rightarrow -\frac{1}{2}$ transition of Fe^{3+} as a function of the direction of the magnetic field in the (110) plane, for three different temperatures: $T=300°K$, $T=77°K$, and $T=1.3°K$. The unexplained angular dependence remains qualitatively the same versus temperature, but quantitatively there is a decrease in going from room temperature to liquid-nitrogen temperature, and a subsequent increase again on going further down to liquid-helium temperatures.

The origin of the linewidths of Mn^{2+} and Fe^{3+} in MgO, then, has been firmly established in the case of the fine structure transitions (as shown in Sec. IIIA), but remains a puzzle in the case of the central lines.

IV. EXPERIMENTAL APPARATUS AND TECHNIQUES

A. The Microwave Spectrometer

The microwave spectrometer with which the experiments were done, operates at X band and conforms closely to the description and discussion given by Feher[18] of systems using superheterodyne detection. The system uses magnetic-field modulation and achieves frequency stability by locking the klystron frequency to that of the external resonant cavity that contains the paramagnetic sample; in this fashion, the signals observed are proportional to the derivative of the absorption, $d\chi''/dH$. The magnetic field is measured using the nuclear magnetic resonance of a proton probe which is observed simultaneously with the electron spin resonance by recording both signals in different channels of the same recorder.

B. The Uniaxial Stress Assembly or Squeezer

This part of the apparatus is based on the "perpendicular squeezer" first used and described by Wilson and Feher,[19] and it is shown in Fig. 13. It operates by applying the external stress to the resonant cavity; the stress will then be transmitted to the crystal sample that is properly mounted inside the cavity. During the experiments, the values of the applied stress were read off the scale of the spring; this scale had previously been calibrated as described below:

The absolute magnitude of the stress applied on the crystalline sample was determined by means of two strain gages (Baldwin-Lima-Hamilton FAB 28-S9) cemented (with Eastman Adhesive 910) one on each of the broad faces of a typical MgO sample. (By the use of two strain gages, rather than just one, we were able to monitor gradients in the pressure applied to the sample.) The strain gages operate by showing a change in their characteristic resistance value that is proportional to the pressure they support. These changes are ≈ 1 part in 10^4 for the pressures we use, and they were observed by means of two Wheatstone bridges whose outputs were amplified and fed to a double-channel recorder. The gages were first calibrated by placing known weights on the crystal sample and observing the corresponding changes in the resistances of the gages. Then, the sample was mounted in the squeezer and the changes in resistances in the gages were noted as a function of the stress read off the spring scale. No hysteresis was observed.

The stress experiments were done at 77°K. This allowed us to work with a comfortable signal-to-noise ratio and also provided a reliable mounting of the crystal. In fact, if the system is prestressed before cooling, then the cardboard "cushions" will distort to accommodate the crystal and then freeze in this state. Any changes in the state of stress of the system after that will result in virtually no change in size of the cavity: the resonant frequency will change by only 0.5 Mc/sec per 100 kg/cm². This change in frequency was used as an additional monitor of the relative pressures applied during the experiment; it is extremely reproducible and leads to an error due to randomness in applied pressure $<1\%$.

C. The Samples

In choosing MgO as the host material in which to carry out these experiments, the guiding considerations were the following: It possesses a simple lattice structure, amenable to direct interpretation when distorted by stress; it incorporates paramagnetic impurities easily; it possess good mechanical qualities such as lack of buckling under stress, and rigidity (a test sample normally mounted in the squeezer reached its breaking point somewhat above 2000 kg/cm²).

---

[18] G. Feher, Bell System Tech. J. 26, 449 (1957).

[19] D. K. Wilson and G. Feher, Phys. Rev. 124, 1068 (1961).

necessary cuts with a diamond wheel at 45°. In mounting the crystal in the resonant cavity it would be desirable to have samples that are long enough to dispense with the quartz spacers. In practice, however, the blocks of MgO we start out from are not large enough to permit this.

APPENDIX: ORIGIN AND ESTIMATE OF THE EXPERIMENTAL ERRORS IN THE DETERMINATION OF THE STRESS COEFFICIENTS

A. Sources of Experimental Errors

1. Magnitude of the pressures applied. The accuracy to which the pressure applied to the crystalline sample is known, is $\pm 3\%$. This represents a systematic error due to uncertainty in the calibration of the strain gages.

2. Orientation of the sample. Deviations from the ideal stressing configuration will occur if the sample is rotated around the [001] axis, or the [1$\bar{1}$0] axis, by an angle which we shall call γ.

Deviations by rotation around the [001] axis will occur if the upper and lower sides of the crystal are not cut accurately, or if the inside walls of the cavity are slanted. We estimate that these deviations amount to less than 0.5°.

Orientation of the magnetic field along a known direction in the (110) plane is achieved by rotating the magnet, whose base is provided with an angular scale and vernier. If we can "zero" this scale by knowing one crystalline direction in the (110) plane, it is possible to obtain any other by rotation. We find we can zero the scale along the [001] direction to $\sim$0.1° by making use of the symmetry of the spectrum of Fe^{3+} (or Mn^{2+}) around the inflection point along the [001] (see Fig. 4).

Misorientation due to rotation around the [1$\bar{1}$0] axis can be estimated from the pressure gradients it introduces. These gradients manifest themselves in an increase under stress of the paramagnetic resonance linewidths of the fine structure of Mn^{2+} and Fe^{3+} since

FIG. 13. Schematic drawing of the mechanical assembly used to apply uniaxial stresses. The spring pulls on a copper wire which, in turn, pulls on a lever arm that transmits the force to the cavity holder and hence to the cavity. The insert shows the details of the mounting of the crystal sample inside the microwave cavity. The assembly of sample plus quartz spacers is slightly longer than the inside dimension of the cavity. The external load is applied to the boss and transmitted to the crystal via the hinging action of the cavity at the Teflon strip. Not shown is the Styrafoam that fills the free volume of the cavity to keep the various parts in place during assembly.

The samples used for the stress experiments were obtained from Norton Company. They contain varying amounts of Mn^{2+}, Fe^{3+}, V^{2+}, Ni^{2+}, Cr^{3+} in the range of 10^{17} to 10^{18} paramagnetic centers per cc.

As we explained previously, the samples used in the stress experiments had to be cut with edges parallel to the [001], [110], and [1$\bar{1}$0] axes so the external stress could be applied along the [110] axis. Since the MgO crystals can be cleaved very well in the planes of the cubic axes, the procedure used was to cleave a thin slab of material and two of its sides and then make the

the linewidth of these transitions is due to random stresses built into the crystal; if these lines broaden under stress, it is due to an additional distribution of stresses being introduced. In a run with a carefully mounted sample the stress broadening of a line is characteristically 30% of its stress shift.

What tilt angle will give rise to gradients of this magnitude? This can be estimated from the determinations made with two strain gages cemented to the sample. By playing very delicately with the positioning of the sample, it is possible to eliminate the difference in reading between both gages. That is, it is possible to eliminate the gradients introduced to within the accuracy of our measurement. These gradients, however, are extremely sensitive to tilts in the sample. Thus, deviations from the "straight" position that are not visually detectable will introduce gradients $\approx 30\%$ from face to face of the sample. In terms of the dimensions of the MgO sample used in these determinations, we estimate the tilt to be

$$\frac{\frac{1}{4} \text{ the narrowest dimension of the sample}}{\text{length of the sample}} = \frac{0.2 \text{ mm}}{20 \text{ mm}}.$$

This yields a deviation γ of less than $1°$.

What is the error in the stress coefficients due to a misalignment $\gamma = \pm 1°$ around the $[1\bar{1}0]$ axis? We can estimate this explicitly using Eq. (2). The pressure P now lies off the $[110]$ axis by an amount γ, small enough so we can set $\cos \gamma = 1$ and $\sin \gamma = \gamma$. Its components in the cubic system, then, are $X_{11} = X_{22} = X_{12} = \frac{1}{2}P$; $X_{33} = \gamma^2$; $X_{13} = X_{12} = X_{23} = -2^{-1/2}\gamma P$. If now $H \| [1\bar{1}0]$, then

$$\delta H_{3/2 \to 1/2} = 3P\{\tfrac{1}{4}C_{11}(1 - \tfrac{1}{2}\gamma^2) - \tfrac{1}{2}C_{44}\};$$

the error depends quadratically on γ and is $\approx 0.05\%$. If $H \perp [110]$ and also $\perp P$ (i.e., H is off being $\|[001]$ by γ), then

$$\delta H_{3/2 \to 1/2} = -3P\{\tfrac{1}{2}C_{11}(1 - 5/4\gamma^2) - C_{44}\gamma^2\};$$

the error again depends quadratically on γ and is $\approx 0.05\%$. If, however, $H \perp P$ and $55°$ off $[001]$ (i.e., H is slightly off being $\|[111]$), then

$$\delta H_{3/2 \to 1/2} = \tfrac{3}{4}C_{11}P(\sqrt{2}\gamma + \tfrac{1}{2}\gamma^2) + C_{44}P(1 - \sqrt{2}\gamma + \tfrac{1}{2}\gamma^2)$$

+higher order terms in γ; the error depends now linearly on γ and is $\approx 5\%$.

If possible, therefore, it is best to choose $H \| [001]$ and $H \| [1\bar{1}0]$ as the two directions along which observations are to be made to determine C_{11} and C_{44}. The error in these constants due to misorientation will be of the order 0.1% and negligible compared to the other sources of error. However, in the case of C_{44} of Fe^{3+} which is determined with $H \| [111]$ (as explained in Sec. IIB), the error due to misorientation will be $\pm 5\%$.

3. Determination of the center of a line. The limitations to the accuracy with which we can determine the center of a line of width ΔH, are the asymmetries in the line shape and the signal to noise of the trace analyzed.

The usual source of asymmetry is admixture into a $d\chi''/dH$ trace, of some amount of signal proportional to dispersion $d\chi'/dH$. With the external cavity stabilization scheme (see Sec. IV), the asymmetry due to admixture of dispersion is at worst 1%. Calling δH the discrepancy between the central crossing of the abscissa of the asymmetric line and the crossing or true center of the perfectly symmetric line, we estimate $\delta H/\Delta H \approx 1\%$.

If we now consider the line to be perfectly symmetric there is still some error involved in determining the central crossing because of noise. In our experiments, the ratio signal/noise ≈ 100 so that $2\delta H/\Delta H \approx 1\%$.

b. Evaluation of the Experimental Error in the C_{ij}

1. Random errors. These are the errors in determining the shift of a line under stress, and the random errors in the increments in pressure. The former are due to the determination of the center of the lines from which the shifts are obtained, and have been estimated to be $\pm 2\%$ of the shifts measured. In the absence of other errors, this alone yields $\pm 1\%$ in the C_{ij}, and fully accounts for the spread of the experimental points in the plots of Figs. 6 and 7.

2. Systematic errors. These are due to uncertainty in the total pressure applied and to misorientations. Errors due to misorientation only become important in the case of C_{44} of Fe^{3+}. They were estimated to be $\pm 5\%$ and must be added to 3% error in pressure giving a total systematic error of 6%. The other three stress coefficients have a total systematic error of 3%.

The total errors will be given by the independent addition of the systematic and random errors, yielding 6% in C_{44} for Fe^{3+} and 3% in the other three stress coefficients.
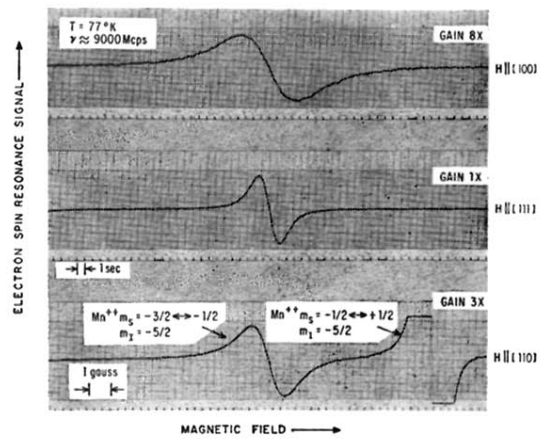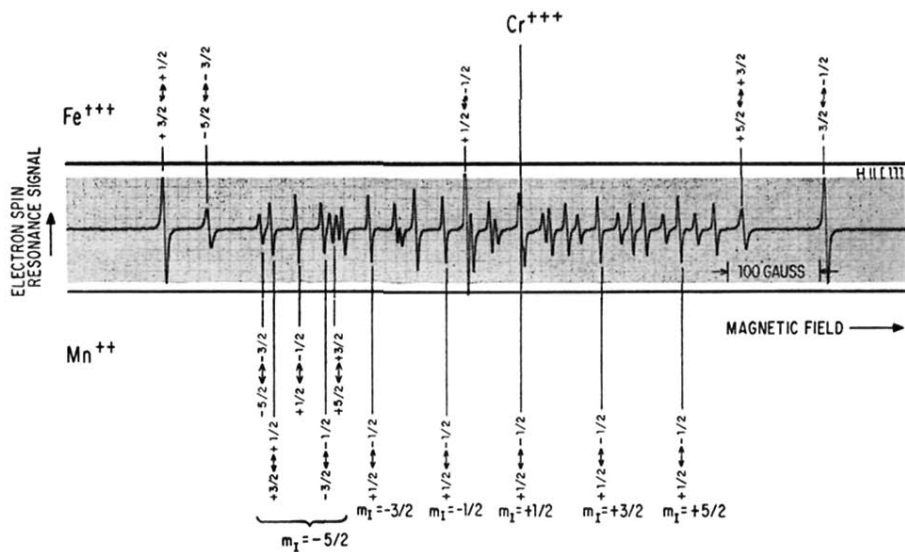
FIG. 11. Change in width of the electron spin resonance line observed for three different directions of the magnetic field; $T = 77°$K and $\nu \approx 9000$ Mc/sec. The traces depict the Mn^{2+} transition, $m_s = -\frac{3}{2} \rightarrow -\frac{1}{2}$, $m_I = -\frac{5}{2}$, but all of the fine structure lines of Mn^{2+} or Fe^{3+} show a similar behavior.

FIG. 2. Typical electron spin resonance spectrum of paramagnetic impurities in MgO, observed at 77°K and with $H\|[111]$ axis ($\nu_e \approx 10\,000$ Mc/sec). The complexity of the spectrum is due mainly to the thirty transitions of Mn^{2+}. For the orientation shown, the Mn^{2+} lines are flanked at both ends of the spectrum by the Fe^{3+} fine structure; at other angles, the Fe^{2+} fine structure approaches the central transition near $g=2.00$ and so merges into the M^{2+} spectrum. A certain amount of Cr^{3+} is almost always present in these samples; its resonance signal is only partially resolved from the central, $m_I=+\frac{1}{2}$, Mn^{2+} line in the trace shown.
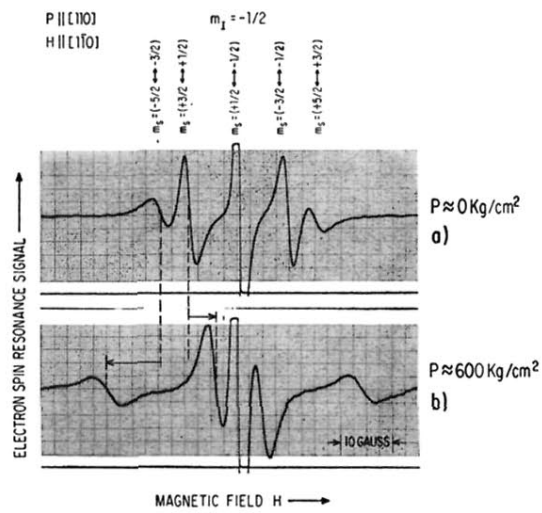
FIG. 3. Electron spin resonance signal of the $m_I = -\frac{1}{2}$ pentad of Mn^{2+}, observed with $H\|[1\bar{1}0]$ and $P\|[110]$ at 77°K. (a) shows and labels the electronic transitions in the absence of external stress. (b) shows the displacement of the transitions when $P \approx 600$ kg/cm²; the lines $m_s = -\frac{5}{2} \rightarrow -\frac{3}{2}$ and $m_s = -\frac{3}{2} \rightarrow -\frac{1}{2}$ shift to lower fields and the other two lines to higher magnetic fields. Also the $m_s = \pm\frac{5}{2} \rightarrow \pm\frac{3}{2}$ transitions shift more than the $m_s = \pm\frac{3}{2} \rightarrow \pm\frac{1}{2}$ lines.